

An Efficient Method for Determining Capillary Pressure and Relative Permeability Curves from Spontaneous Imbibition Data

Mojtaba Ghaedi^{1*}, Zoltán E. Heinemann², Mohsen Masihi³, and Mohammad Hossein Ghazanfari⁴

¹ PhD Candidate, Department of Chemical and Petroleum Engineering, Sharif University of Technology, Tehran, Iran

² Professor, Montanuniversitaet Leoben, Franz-Josef-Strasse 18, 8700 Leoben, Austria

³ Associate Professor, Department of Chemical and Petroleum Engineering, Sharif University of Technology, Tehran, Iran

⁴ Assistant Professor Department of Chemical and Petroleum Engineering, Sharif University of Technology, Tehran, Iran

Received: August 21, 2014; revised: April 07, 2015; accepted: May 28, 2015

Abstract

In this paper, a very efficient method, called single matrix block analyzer (SMBA), has been developed to determine relative permeability and capillary pressure curves from spontaneous imbibition (SI) data. SMBA mimics realistically the SI tests by appropriate boundary conditions modeling. In the proposed method, a cuboid with an identical core plug height is considered. The equal dimensions of the cuboid in x and y directions are set such that the cylindrical core plug and the cuboid have the same shape factor. Thus, by avoiding the difficulties of the cylindrical coordinates, a representative model for the core plug is established. Appropriate grid numbers in x - y and z directions are specified to the model. Furthermore, the rock and fluid properties of SI test are set in the SMBA. By supposing forms of the oil-water capillary pressure and relative permeability and comparing the oil recovery curves of SMBA and SI data, capillary pressure and relative permeability can be determined. The SMBA is demonstrated using three experimental data with different aging times. Suitable equations are employed to represent the capillary pressure and relative permeability curves. The genetic algorithm is used as the optimization tool. The obtained results, especially for capillary pressure, are in good agreement with the experimental data. Moreover, the Bayesian credible interval (P10 and P90) evaluated by the Neighborhood Bayes Algorithm (NAB) is quite satisfactory.

Keywords: Spontaneous Imbibition, Single Matrix Block Analyzer, Recovery Curve, Genetic Algorithm, Neighborhood Bayes Algorithm

1. Introduction

Oil-water capillary pressure and relative permeability are significant data in reservoir engineering (Li et al., 2005; Hou et al., 2012). Centrifuge, steady-state, and unsteady displacement techniques are frequently employed to determine the relative permeability data (Honarpour et al., 1986). Capillary pressure is verified regularly using porous-plate, centrifuge, and mercury-injection methods (Li et al., 2005). Each of these experimental methods has its own advantages and disadvantages. Unsteady-state

* Corresponding Author:
Email: mojtaba.ghaedi@gmail.com

techniques for low permeability rocks encounter problems and steady-state methods are time consuming (Schembre and Kovscek, 2006; Hou et al., 2012). The porous-plate and centrifuge methods sometimes cannot be used for core samples with a very low permeability and mercury injection technique cannot represent the actual reservoir fluids (Li et al., 2005).

For studying matrix-fracture communication, SI tests, especially counter-current SI tests, are of great importance (Haugen et al., 2014; Pooladi-Darvish, Firoozabadi 2000). It would be quite advantageous to determine the relative permeability and capillary pressure curves from relatively simple, fast, and economical counter-current SI tests (Li et al., 2005; Haugen et al., 2014; Schembre and Kovscek, 2006). Additionally SI tests are much more close to the reality of the naturally fractured reservoirs; thus the acquired relative permeability and capillary pressure curves based on SI results are more reliable to study oil recovery in water invaded zones.

There are few studies on deriving oil-water capillary pressure and relative permeability from SI data. Bourbiaux and Kalaydjian (1990) used 1-D finite-difference numerical model to simulate the flow behaviors during co-current and counter-current SI tests. They reported that the relative permeabilities resulted in a good prediction of countercurrent oil recovery rate are about 30% less than the co-current relative permeabilities at a given water saturation. Behbahani et al. (2006) simulated counter-current imbibition by using a commercial simulator and generating 1D or 2D fine grids. They compared the results with experimental measurements in the literature. Li et al. (2005) proposed a method to infer the capillary pressure and the global mobility data from SI experiments in oil-saturated rock. The presented approach lies on the plot of calculated imbibition. In their method, the relative permeability of one phase has to be known to be able to determine the relative permeability of another phase. Schembre and Kovscek (2006) used recorded water phase saturation profiles during SI by X-ray computerized tomography scanning to estimate simultaneously capillary pressure and relative permeability. In their method, the simulated annealing optimization was used and they quantified non-equilibrium effects during SI. Special boundary conditions were described by Haugen et al. (2014), in which co-current and counter-current flow can occur simultaneously. In the suggested method, for the period after the cessation of counter-current production, the relative permeability behind the front and the effective capillary driving pressure at the front can be estimated. The presented method needs enough production data points to be certain and therefore long samples are required for experiments. Other modeling efforts in this area are based on some simplifying assumptions (Putra et al., 1999; Chen et al., 1995) or restricted to 1D flow (Blair 1964; Kashchiev and Firoozabadi 2003).

A method has been developed herein which determines oil-water relative permeability and capillary pressure functions based on oil recovery curve of the SI test. The proposed method was called SMBA. This approach simulates the SI process in a plug size model. The simulation method is a fully implicit control volume finite difference method. By correct handling of plug boundary conditions during SI experiment, SMBA models the process more accurately. The applicability of the SMBA to three available experimental data with different aging times is also presented. Consistent equations for relative permeability and capillary pressure were employed. In addition, the combination of GA and NAB algorithm were utilized for optimization and uncertainty quantification.

2. Experimental data

Cores used for SI test were cut with the same orientation from a sandstone outcrop. The prepared core plugs have almost similar properties (Table 1). It should be emphasized that there were no fractures in the cores utilized for the imbibition tests. Table 2 illustrates the properties of the crude oil and

synthesis brine used as the fluids during the SI experiments. The interfacial tension between the brine and the crude oil was 30 dyne/cm measured by ring tensiometer. The brine contains NaCl, KCL, and CaCl₂.H₂O mixed with distilled water (Heinemann 2013).

The core plugs were washed and first dried at ambient temperature, and then oven dried at 100 °C. The dried core plugs were vacuumed and saturated with the brine. By measuring the change in weight, the porosity was calculated. Permeability to brine was determined by means of a biaxial core holder. Then, by the injection of the crude oil, the initial water saturation (S_{wi}) of about 25% was established in the cores. Afterwards, the core was aged in the crude oil at 90 °C for 72 and 240 hours (Table 1). For each aging time (0, 72, and 240 hours), 3 core plugs were considered as the backup. Standard steady-state (Figure 1) and centrifuge methods (Figure 2) were used to determine relative permeability and capillary pressure respectively. Finally, the SI tests were performed using imbibition apparatus (Figure 3) at room temperature. It should be emphasized that the aging time necessary to re-establish the reservoir differs depending on the crude, brine, and reservoir rock. Generally, it should be aged for 1,000 hours (40 days) at the reservoir temperature (Anderson 1986). Since the purpose of this work was not to restore the reservoir wettability, the aging time was shorter herein.

Table 1

The parameters of cores used in the SI tests.

Sample	Aging Time (hrs)	L (cm)	d (cm)	K (md)	ϕ (%)	S_{wi} (%)
1	0	8.51	3.5	135	0.21	0.25
2	72	8.50	3.5	134	0.208	0.25
3	240	8.50	3.5	135	0.212	0.26

Table 2

Properties of fluids used in the SI tests at 20 °C.

Fluid	Viscosity (cP)	Density (kg/m ³)
Brine	1	1010
Crude Oil	2.4	730.8

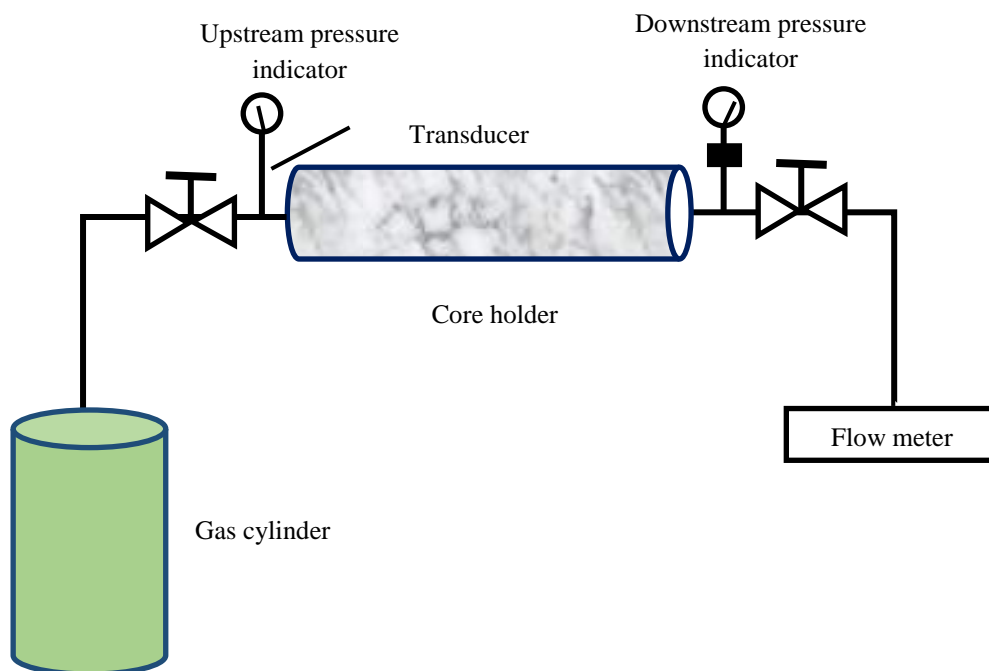


Figure 1
Experimental setup for measuring steady-state relative permeability.

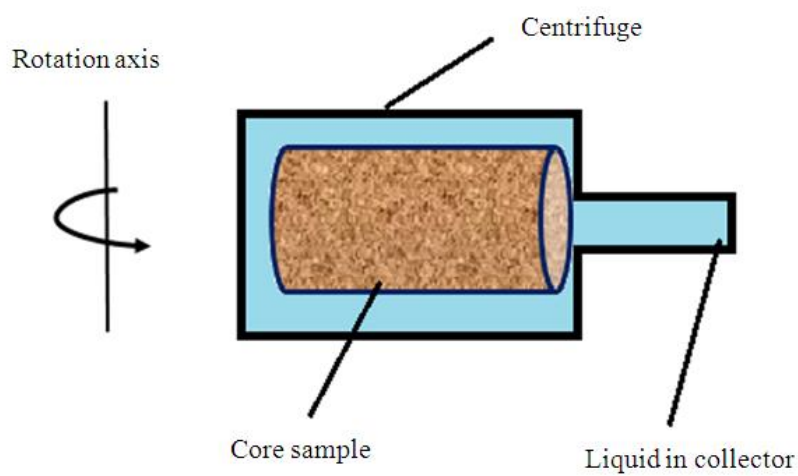
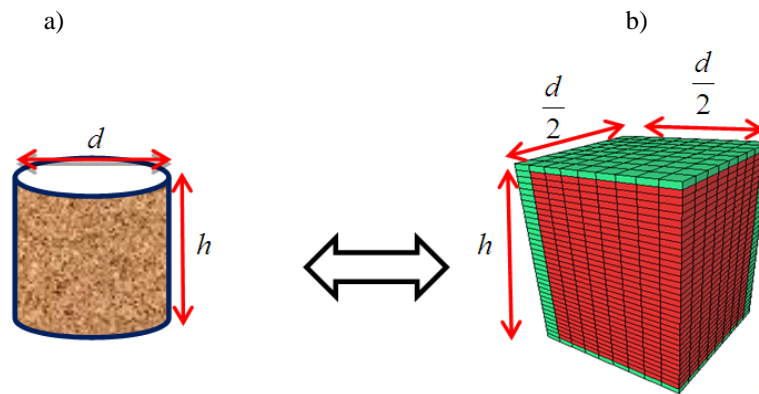


Figure 2
Experimental apparatus setup for determining capillary pressure.

**Figure 3**

(a) Counter current imbibition test setup; (b) A quarter of the simulation model, illustrating matrix blocks (red blocks) and surrounding fractures (green blocks).

3. Description of SMBA

Simulation of a matrix block surrounded with fractures and generation of recovery curves may encounter with several challenges, including numerical instability and unrealistic modeling. Numerical instability problems originate from very small pore volumes of the grid cells, especially for the fracture cells, high permeability contrast between matrix and fracture cells, and the necessity to use bottom hole pressure controlled wells. The difficulty to handle boundary conditions can cause the unrealistic modeling of imbibition test and the determination of recovery curve. A proper simulation of imbibition test requires assuring constant pressure and saturations in the core boundaries.

The SMBA was developed as an auxiliary option in the available research code. SMBA run is similar to a typical reservoir model run. The rock and fluid properties are determined for the model. Then, a simplified model, a single matrix block surrounded by fractures, will automatically be generated and gridded. Selecting the right grid in the numerical modeling is always a challenge. Because the correct balance between the grid resolution and acceptable simulation run time has to be found, Pirker et al. (2007) made a sensitivity analysis and found that the optimal grid block number for the matrix was $8 \times 8 \times 36$ (Figure 4). Fracture planes are added to the matrix block to finalize the simulation grid. The fracture planes surrounding the matrix block can be set in all directions or just in the vertical direction. Therefore, different boundary conditions for the matrix block can be simulated. The results of the SMBA for water displacement were verified by comparing the results with analytical Buckley-Leverett theory solution (Pirker et al., 2007). The simplifying assumptions of the Buckley-Leverett theory were applied to the SMBA model (Buckley and Leverett 1942). Figure 5 compares the SMBA and analytical runs.

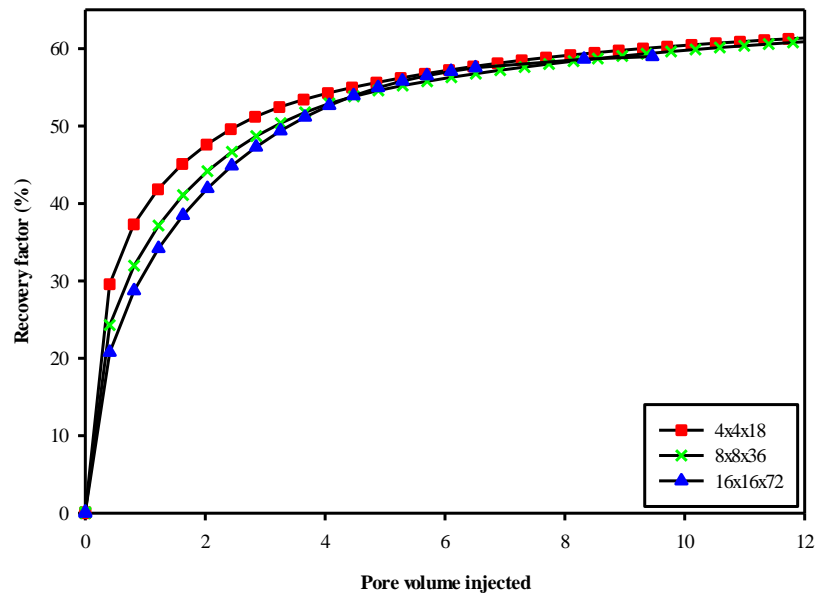


Figure 4
Sensitivity analysis of grid numbers of the matrix block (Pirker et al., 2007).

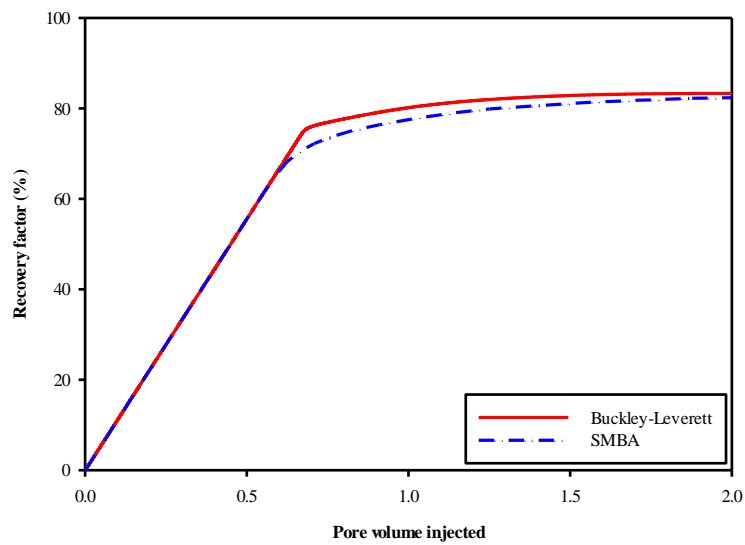


Figure 5
Comparison of Buckley-Leverett and SMBA solutions in a simplified water displacement model.

Because of symmetry, only a quarter of the model is calculated in the SMBA; the side length of the cube is reduced in x - and y -direction to half. To maintain the gravity force, the dimension in z -direction remains the same. Oil displacement in the matrix block during the SMBA run is shown in Figure 6.

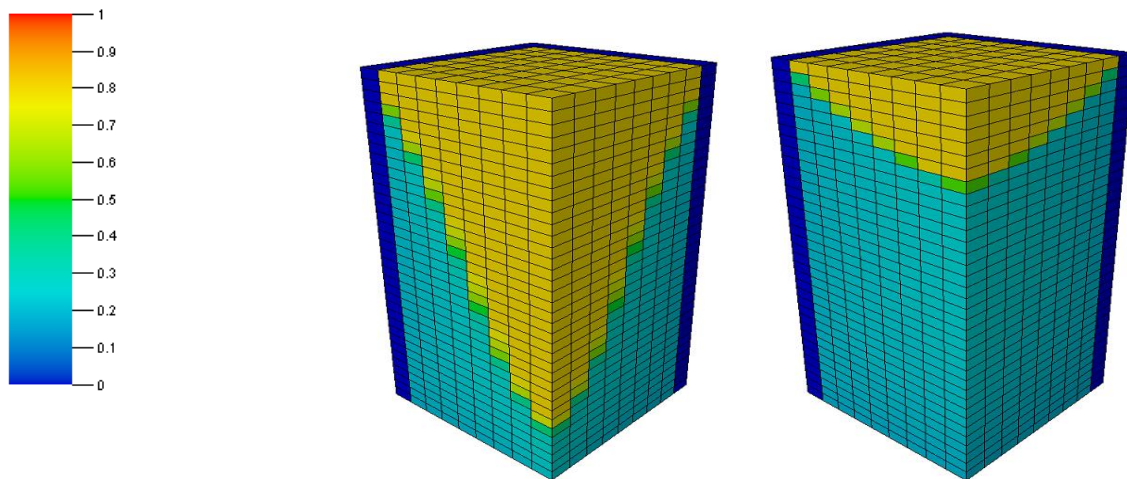


Figure 6

Oil saturation distribution in a quarter of the matrix block with surrounding fractures during the run with SMBA.

Regarding the single matrix block with its boundaries, three types of inter-cell transmissibilities can be considered:

1. Matrix-matrix: this is the single-porosity transmissibility between the matrixes. It should be noted that, since all the cells are of the same size (and with the same parameters), the value of transmissibility in each direction is the same for all the matrix cell pairs.
2. Boundary-boundary: since the flow in the boundary blocks is unimportant and the contents of the boundary blocks will always be restored to the initial state, the boundary-boundary transmissibility is by default set to zero to prevent the uninteresting flow between the boundary blocks. The reason is to make the simulation of the imbibition process very close to the reality. Also, in the SI tests, the saturations of the boundaries of the cores change very fast and restore to the unit saturation.
3. Matrix-boundary: the transmissibility is calculated as in the single porosity model but by only considering the matrix cell length and permeability (since the surrounding cells act just as a boundary to the matrix cells).

The boundary medium has no capillary pressure and straight-line relative permeabilities are given to it. The surrounding cells act just as a boundary to the matrix cells and they are not contributed to the flow. The volume of the boundary cells is set large enough so that they can occupy the oil flowing out from the matrix cells.

4. Application of SMBA to simulating SI tests

SMBA is a very efficient tool to simulate the imbibition tests, i.e. to model the process of oil recovery of a core sample saturated by oil and displaced by water. It credibly models the boundary conditions of the core. In SMBA, at the end of each time-step, the oil content of all of the boundary cells is removed and reported as the amount of the extracted oil. Then, the fracture dynamic properties are set back to their initial value. In this way, the problem of constant bottom hole pressure wells is avoided as well. An effective time-step control and Newton-Raphson iteration method has been implemented, which helps achieve a much better stability.

Core plugs are often in cylindrical shape. The simulation of cylindrical models has its own difficulties and challenges. Therefore, to avoid these problems, cuboid matrix block model is generated with the same height as the core plug. The side directions are selected so that the matrix block model and the core plug have the same shape factor value (2.67 cm^{-2}). Then, the resulting recovery curves of these two models will be the same. Equation 1 describes the generalized shape factor relation (Kazemi et al., 1992):

$$\sigma = \frac{1}{V_b} \sum_{i=1}^n \frac{A_i}{x_i} \quad (1)$$

where, σ is the shape factor, V_b is the bulk volume of the matrix block, and A_i stands for the surface area open to imbibition in the i^{th} direction; x_i is the distance from A_i to the no flow boundary and n represents the number of the surfaces open to flow. Based on Equation 1, to obtain the same shape factor for the two models, if the matrix block is given the core plug height, h , the size of its sides has to be set to the same core plug diameter (d) (Figure 3).

If the small cell sizes of the single matrix block make numerical problems, higher pore volumes can be given to the cells of the matrix block. To obtain relative permeability and capillary pressure relations, instead of matching the recovery curve versus time, scaled recovery curves can be matched. In the most of the previously developed scaling relations, dimensionless time, t_D , is inversely proportional to the square root of the porosity (Ma et al., 1997; Mattax and Kyte, 1962; Zhang et al., 1996; Mirzaei-Paiaman and Masihi, 2013; Schmid and Geiger, 2013; Pordel Shahri et al., 2012); for example, the following equation may be used (Ma et al., 1997):

$$t_D = \sqrt{\frac{K}{\varphi}} \frac{\delta}{\mu_w \mu_{nw} L_c^2} t \quad (2)$$

In this equation, t , L_c , K , and φ are imbibition time, a characteristic length, permeability, and porosity respectively. δ stands for interfacial tension between the phases and μ_w and μ_{nw} are the viscosities of the wetting and non-wetting phases respectively. Thus if higher pore volume is assigned to the matrix block to avoid stability problems, except for porosity, the other parameters of the t_D for the single matrix block model and core plug are the same. Therefore, if the right capillary pressure and relative permeability functions are set in the SMBA, the plots of oil recovery versus $t\varphi^{0.5}$ for the simulated and experimental SI are matched.

5. Formulations

5.1. Capillary pressure

Many capillary pressure correlations have been recommended in the literature; Skjaeveland et al. (2000) developed a general capillary pressure correlation:

$$P_c = \frac{C_w}{\left(\frac{S_w - S_{wR}}{1 - S_{wR}}\right)^{a_w}} + \frac{C_o}{\left(\frac{S_o - S_{oR}}{1 - S_{oR}}\right)^{a_o}} \quad (3)$$

where, S_w is water saturation and S_o is oil saturation; C_w and C_o are the entry pressures for oil and water respectively; $1/a_w$ and $1/a_o$ represent the pore size distribution indexes; S_{wR} stands for irreducible water saturation and S_{oR} denotes residual oil saturation. There is one set of C_w , a_w , C_o , and a_o for imbibition and another for drainage. C_o is a negative number and the other constants are positive. In a completely water-wet system, C_o is zero (Skjæveland et al., 2000).

5.2. Relative permeabilities

Two general groups to represent relative permeability curves are the parametric and the non-parametric models. The Corey-type and power-law relations are common parametric models (Hou et al., 2012; Skjæveland et al., 2000). Expressions have also been developed by Skjæveland et al. (2000) to show relative permeability of water and oil:

$$k_{rw} = k_w^* \frac{C_w k_{rw,ww} - C_o k_{rw,ow}}{C_w - C_o} \quad (4)$$

$$k_{ro} = k_o^* \frac{C_w k_{ro,ww} - C_o k_{ro,ow}}{C_w - C_o} \quad (5)$$

In Equations 4 and 5, $k_{rw,ww}$ is the water relative permeability in a completely water-wet system and $k_{ro,ww}$ represents the corresponding oil relative permeability. Additionally, $k_{rw,ow}$ and $k_{ro,ow}$ are water and oil relative permeability in a completely oil-wet medium respectively. Also, k_o^* is oil relative permeability at irreducible water saturation and k_w^* stands for water relative permeability at residual oil saturation.

In a completely water-wet system, the following relations can be written for oil and water relative permeabilities (Skjæveland et al., 2000):

$$k_{rw,ww} = S_{nw}^{3+2a_w}, \quad k_{ro,ww} = (1 - S_{nw}^{1+2a_w})(1 - S_{nw})^2 \quad (6)$$

where,

$$S_{nw} = \frac{S_w - S_{wR}}{1 - S_{wR} - S_{oR}} \quad (7)$$

Similarly in a completely oil-wet system, the following equations can describe oil and water relative permeabilities:

$$k_{ro,ow} = S_{no}^{3+2a_o}, \quad k_{rw,ow} = (1 - S_{no}^{1+2a_o})(1 - S_{no})^2 \quad (8)$$

where,

$$S_{no} = \frac{S_o - S_{oR}}{1 - S_{wR} - S_{oR}} \quad (9)$$

The selected equations for capillary pressure and relative permeabilities have constant parameters in common. This makes the optimization process of finding suitable capillary pressure and relative permeabilities functions more efficient, because less unknown variables have to be determined.

5.3. Objective function

The considered shape of the objective function is illustrated in Equation 10:

$$M = \sum_{i=1}^{N_i} (x^{Exp}(t^i) - x^{Sim}(t^i))^2 \quad (10)$$

where, M is a misfit value and N_i is the number of the measured oil recovery curve to be matched; $x^{Exp}(t^i)$ stands for the experimental value of oil recovery at the corresponding t and $x^{Sim}(t^i)$ represents the simulated amount of oil recovery at the equivalent t .

6. Workflow

The workflow of this paper is made of two steps (Figure 7). In the first step, the oil recovery curve output of the SMBA and SI test were matched. In this step, GA was coupled with the SMBA to determine the best and ensemble of capillary pressure and relative permeability functions. The second step involved the statistical inference of the ensemble of the obtained answers.

MATLAB OptimizationToolbox and the NAB method of Sambridge (1999) have been employed as the optimization tool and statistical analysis respectively. NAB is a subset of the Markov chain Monte Carlo method. This technique builds an approximation for the real posterior probability distribution using a Gibbs sampler. Then, by building a multidimensional interpolator in the model space, information is gathered from an ensemble of the forward solutions. In this way, any Bayesian integral can be evaluated. There is no need for more forward simulations, and thus this method is quite fast. For more information about this method see (Sambridge 1999).

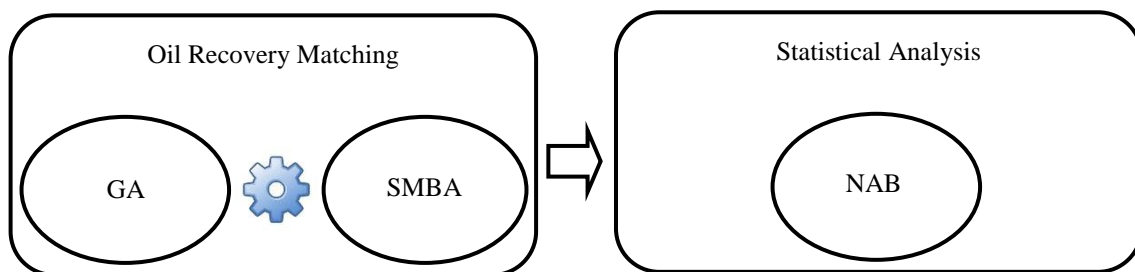


Figure 7
Workflow of the paper, oil recovery matching and statistical analysis.

7. Results and discussion

The matching parameters of the capillary pressure and relative permeability functions were C_w , a_w , C_o , a_o , k_o^* , k_w^* , S_{wR} , and S_{oR} . At first, different combinations of GA parameters were tested. Table 3 shows the selected configuration of the GA parameters. The parameters of the best matched models are tabulated in Table 4. During the optimization process, an ensemble of 964 solutions was obtained. They were submitted to the NAB method for uncertainty quantification.

Table 3
GA parameters used for the matching oil recovery curve.

Population	Maximum no of generation	Cross over type	Cross over Rate	Mutation Rate
40	40	Scattered	0.75	0.04

Table 4
Parameters of the best matched models.

Parameter	0 hr aging time	72 hrs aging time	240 hrs aging time
C_w	1.31	0.78	1.25
a_w	0.21	0.22	0.2
C_o	-0.001	-1.01	-1.7
a_o	0	0.01	0.001
S_{wR}	0.25	0.24	0.27
S_{oR}	0.21	0.31	0.32
k_w^*	0.31	0.35	0.41
k_o^*	0.95	0.92	0.86

Figures 8-14 compare the experimental data with the simulation results. An excellent match between the experimental and the best calculated oil recovery factors for the three core samples can be seen in Figure 8. According to this figure, as expected, the imbibition rate decreases by increasing the aging time (t_a). The reason of the strong effect of the aging time on the data can be interpreted as the fast adsorption of the wettability-altering compounds (polar compound and/or the deposition of the organic matters originally in the crude oil) during the aging process.

Figures 9-11 present the calculated capillary pressure for the three core samples. The best calculated capillary pressures are in good agreement with the experimental data. Furthermore, the Bayesian credible interval (P10 and P90) is acceptable. The credible interval was obtained by submitting the 964 solutions to the NAB method. A Bayesian probability interval, also known as credible interval, includes information from the prior distribution into the assessment. In Bayesian inference, a probability interval is a probabilistic area around a posterior moment and using a probability interval is similar to a frequentist confidence interval. For example, if a statistical method approximates the mean of a_o of a population to be 0.1, with a 90% credible interval of 0.008-0.11, then the estimated posterior probability is that 90% of that population is between 0.008 and 0.11, with a mean of 0.1. These figures also confirm that Equation 3 is general and flexible to represent the capillary pressure curve.

The predicted oil-water relative permeabilities are illustrated in Figures 12-14. The best solutions and the predicted intervals are to some extent acceptable. The Non-parametric models such as cubic B-spline model are more general and flexible (Hou et al., 2012). Using these models to represent relative permeability functions may improve the predicted relative permeability. The reason of using Equations 4 and 5 to depict relative permeability relations is the common unknown parameters of Equation 3 utilized for the capillary pressure curve, because the number of the unknowns, which have to be determined during the optimization step, reduces. This may help avoid non-unique solutions for the relative permeabilities and capillary pressure functions, which is the widespread problem of the inverse problems. Another advantage of using setup Equations 3-5 is the agreement in the shapes of

the resulted relative permeabilities and capillary pressure; for example, both relative permeabilities and capillary pressure curves show that the system is water-wet.

The relative permeabilities of co-current and counter-current processes are not the same (Bourbiaux and Kalaydjian, 1990). This could be another source for the differences of the predicted and experimental relative permeabilities. The experimental procedure to calculate the relative permeability has been the standard steady-state method, while the SI experiments are counter-current imbibition.

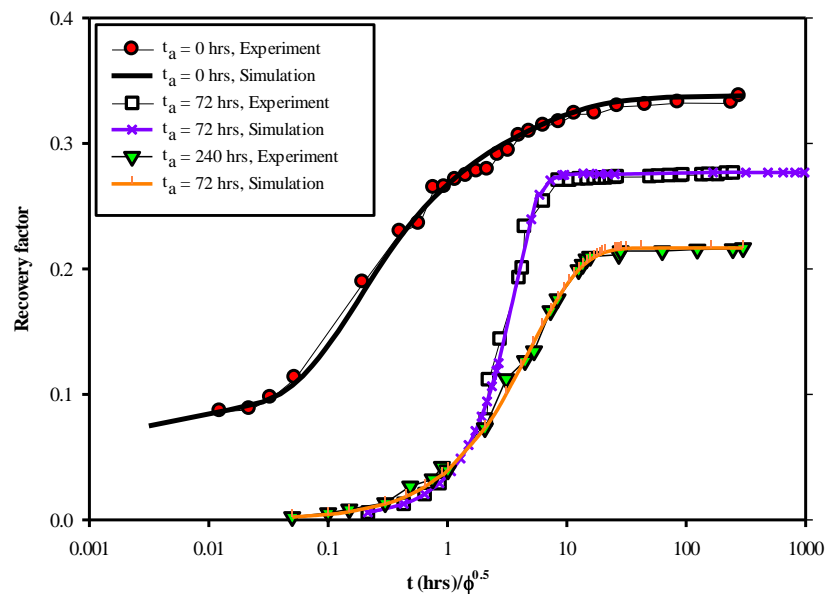


Figure 8

Comparison of the experimental and the best calculated oil recovery factors for the three core samples.

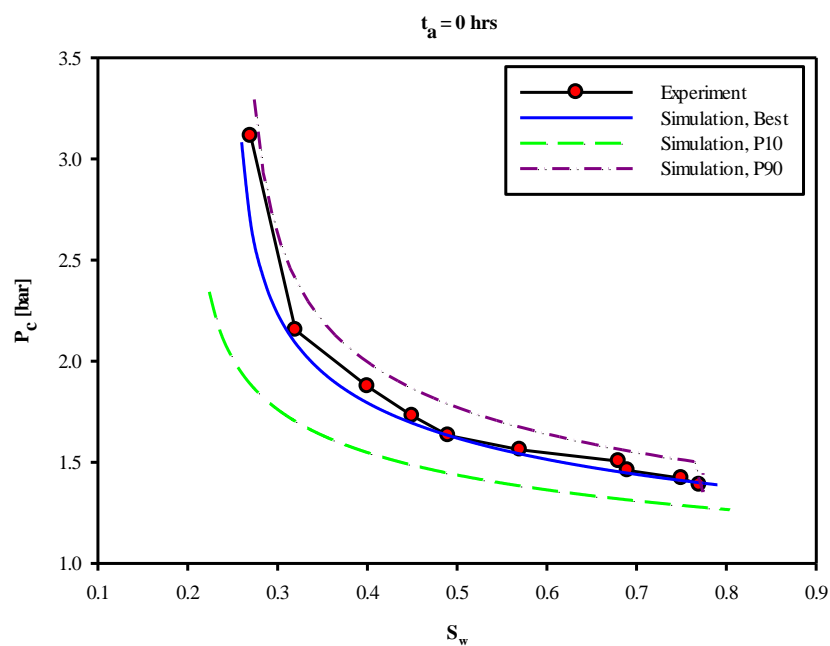


Figure 9

Comparison of the experimental capillary pressure data with the calculated capillary pressure functions (the best and uncertainty interval (P10 and P90)) for the sample with 0 hr aging time.

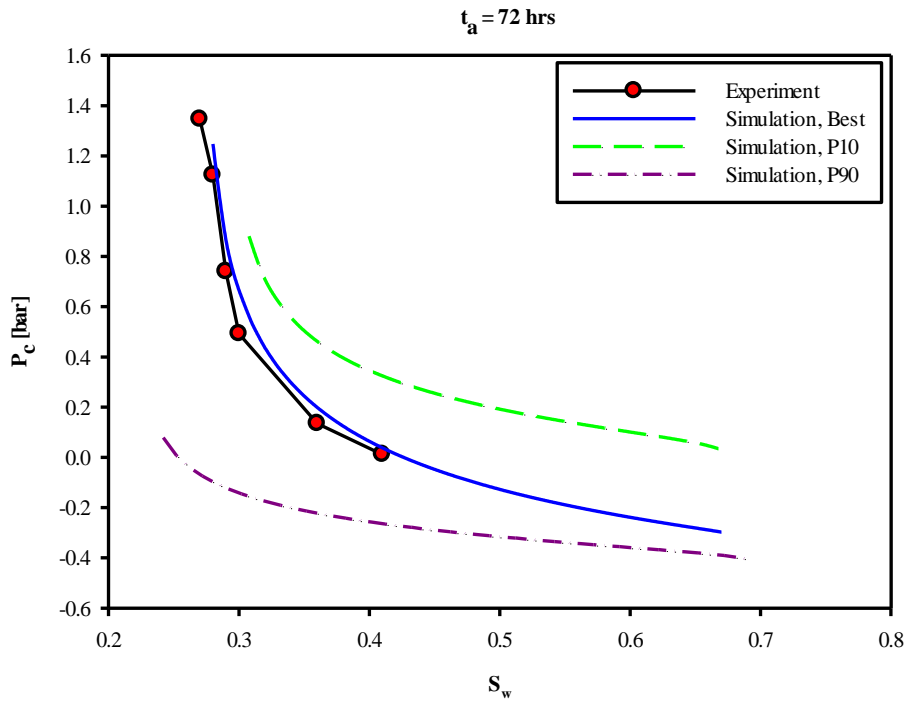


Figure 10

Comparison of the experimental capillary pressure data with the calculated capillary pressure functions (the best and uncertainty interval (P10 and P90)) for the sample with 72 hrs aging time.

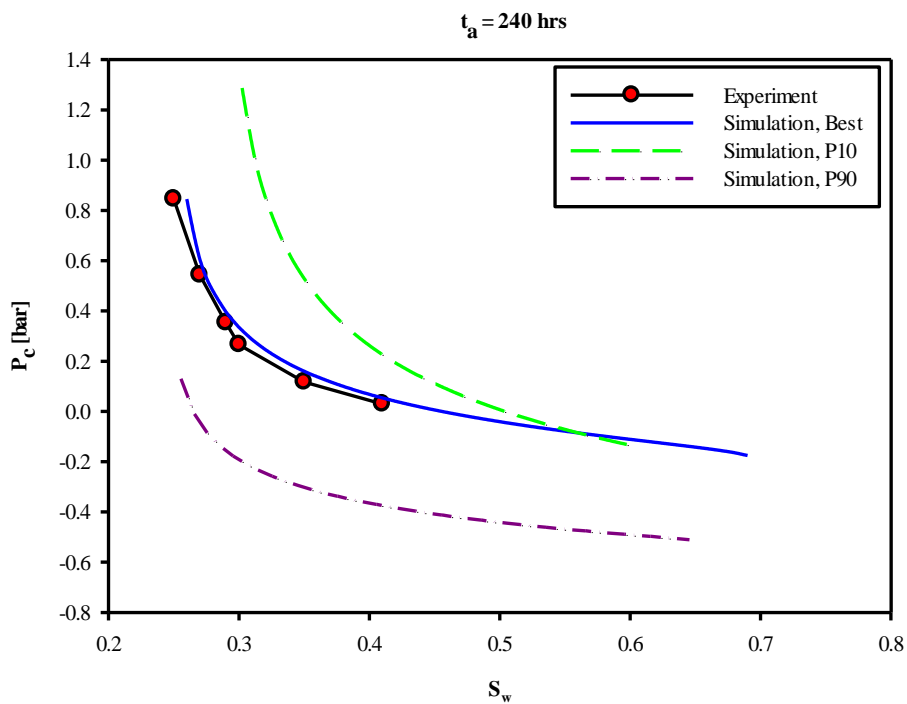


Figure 11

Comparison of the experimental capillary pressure data with the calculated capillary pressure functions (the best and uncertainty interval (P10 and P90)) for the sample with 240 hrs aging time.

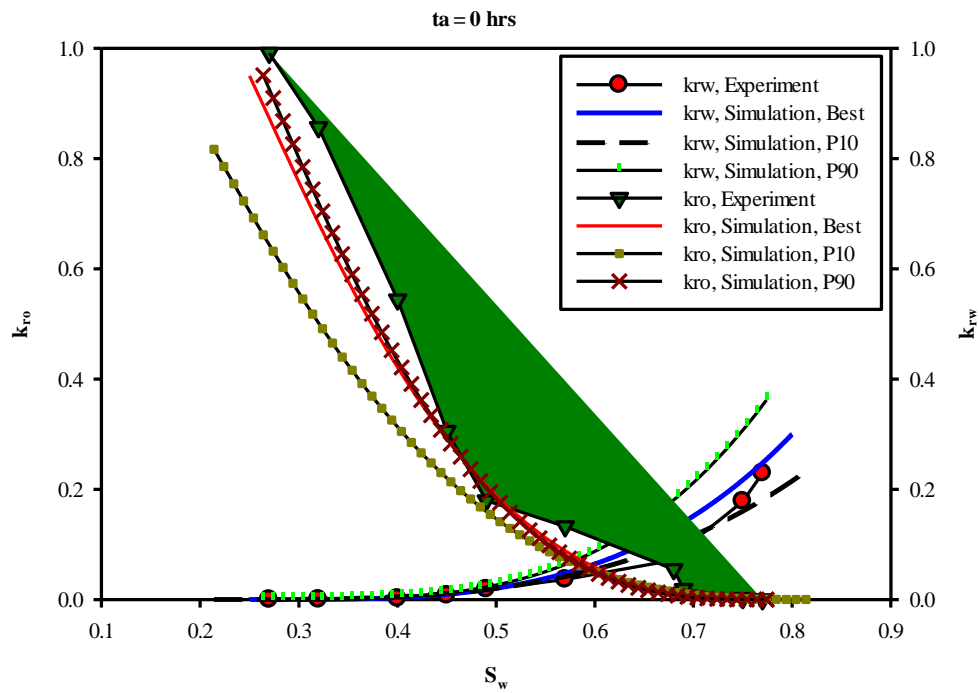


Figure 12

Comparison of the experimental oil-water relative permeabilities data with the calculated relative permeabilities functions (the best and uncertainty interval (P10 and P90)) for the sample with 0 hr aging time.

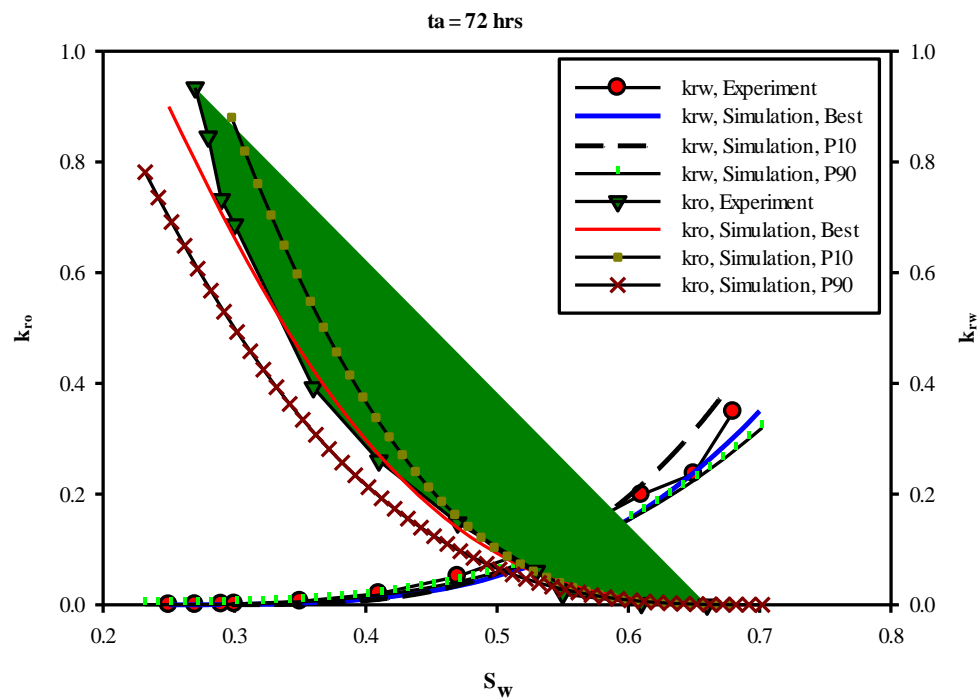


Figure 13

Comparison of the experimental oil-water relative permeabilities data with the calculated relative permeabilities functions (the best and uncertainty interval (P10 and P90)) for the sample with 72 hrs aging time.

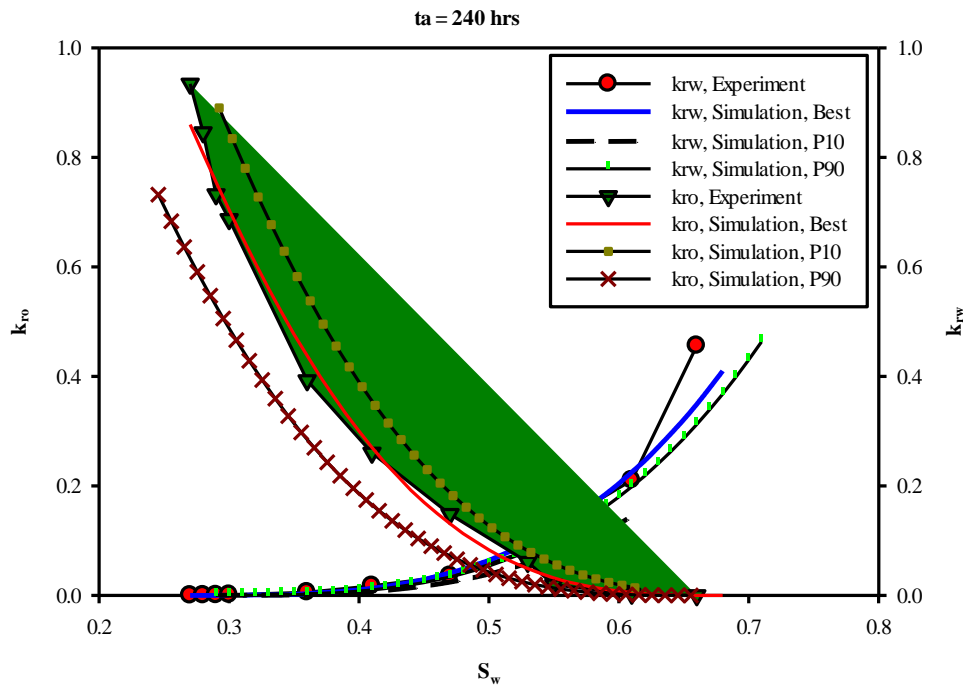


Figure 14

Comparison of the experimental oil-water relative permeabilities data with the calculated relative permeabilities functions (the best and uncertainty interval (P10 and P90)) for the sample with 240 hrs aging time.

8. Conclusions

This paper presented a very efficient method, called SMBA, to infer relative permeability and capillary pressure functions from SI data. The proposed method handles the boundary conditions more reliably, and therefore it simulates the SI tests realistically. In SMBA, a cuboid model with the same core plug height is generated. By assuming the functions of the oil-water capillary pressure and relative permeability and comparing the oil recovery curves of SMBA and SI data, capillary pressure and relative permeability can be determined. The applicability of the method was illustrated on three core samples with different aging times. Appropriate relations were utilized to represent the capillary pressure and relative permeability curves. Moreover, GA was used as the optimization technique. The predicted forms, especially for the capillary pressure curves, are in very good agreement with the experimental data. The Bayesian credible intervals (P10 and P90) predicted by the NAB method are acceptable as well.

Acknowledgements

We wish to thank Prof. M. Sambridge for providing us with his neighborhood algorithm.

Nomenclatures

$1/a_o$: Pore size distribution index for oil
$1/a_w$: Pore size distribution index for water
A_i	: Surface area open to imbibition in the i th direction
C_o	: Entry pressures for water
C_w	: Entry pressures for oil

d	: Core plug diameter
h	: Core plug height
K	: Permeability
k_o^*	: Oil relative permeability at irreducible water saturation
k_w^*	: Water relative permeability at residual oil saturation
$k_{ro,ow}$: Oil relative permeability in a completely oil-wet system
$k_{ro,ww}$: Oil relative permeability in a completely water-wet system
$k_{rw,ow}$: Water relative permeability in a completely oil-wet system
$k_{rw,ww}$: Water relative permeability in a completely water-wet system
L_C	: Characteristic length
M	: Misfit value
n	: Number of the surfaces open to flow
N_t	: Number of the measured oil recovery curve
S_o	: Oil saturation
S_{oR}	: Residual oil saturation
S_w	: Water saturation
S_{wR}	: Irreducible water saturation
t	: Imbibition time
V_b	: Bulk volume of the matrix block
x_i	: Distance from A_i to the no flow boundary
$x^{Exp}(t^i)$: Experimental value of oil recovery at the corresponding t
$x^{Sim}(t^i)$: Simulated amount of oil recovery at the equivalent t
δ	: Interfacial tension
σ	: Shape factor
μ_{nw}	: Viscosity of the non-wetting phase
μ_w	: Viscosity of the wetting phase
ϕ	: Porosity

References

- Anderson, W. G., Wettability Literature Survey- Part 1: Rock/Oil/Brine Interactions and the Effects of Core Handling on Wettability, Journal of Petroleum Technology, Vol. 38, No. 10, p.1125-1144, 1986.
- Behbahani, H. S., Di Donato, G., and Blunt, M. J., Simulation of Counter-current Imbibition in Water-wet Fractured Reservoirs, Journal of Petroleum Science and Engineering, Vol. 50, No. 1, p. 21-39, 2006.
- Blair, P. M., Calculation of Oil Displacement by Countercurrent Water Imbibition, Society of Petroleum Engineers Journal, Vol., 4, No. 3, p.195-202, 1964.
- Bourbiaux, B. and Kalaydjian, F., Experimental Study of Cocurrent and Countercurrent Flows in Natural Porous Media, SPE Reservoir Engineering, Vol. 5, No. 3, p. 361-368. 1990.
- Buckley, S. E. and Leverett, M. C., Mechanism of Fluid Displacement in Sands, Transactions of the AIME, Vol. 146, No. 01, p. 107-116, 1942.

- Chen, J., Miller, M. A., and Sepehrnoori, K., Theoretical Investigation of Countercurrent Imbibition in Fractured Reservoir Matrix Blocks, In Proceedings of SPE Reservoir Simulation Symposium, Society of Petroleum Engineers, 1995.
- Haugen, Å., Fernø, M., Mason, G., and Morrow, N. R., Capillary Pressure And relative Permeability Estimated from a Single Spontaneous Imbibition Test, *Journal of Petroleum Science and Engineering*, Vol. 115, p. 1-12, 2014.
- Heinemann, Z. E., In-house Research Technical Report, Leoben University, 2013.
- Honarpour, M., Koederitz, L., and Harvey, A. H., *Relative Permeability of Petroleum Reservoirs*, C.R.C. Press, Bahman, 1986.
- Hou, J., Luo, F., Wang, D., Li, Z., and Bing, S., Estimation of the Water-oil Relative Permeability Curve from Radial Displacement Experiments Part 1: Numerical Inversion Method, *Energy Fuels*, Vol. 26, No. 7, p.4291-4299, 2012.
- Kashchiev, D. and Firoozabadi, A., Analytical Solutions for 1D Countercurrent Imbibition in Water-wet Media, *SPE Journal*, Vol. 8, No. 4, p.401-408, 2003.
- Kazemi, H., Gilman, J. R., and Elsharkawy, A. M., Analytical and Numerical Solution of Oil Recovery from Fractured Reservoirs With Empirical Transfer Functions (includes Associated Papers 25528 and 25818), *SPE Reservoir Engineering*, Vol. 7, No. 2, p. 219-227, 1992.
- Li, K., Yangtze, U., and Horne, R. N., Computation of Capillary Pressure and Global Mobility from Spontaneous Water Imbibition Into Oil-saturated Rock, *SPE Journal*, Vol. 10, No. 4, p. 458-465, 2005.
- Ma, S., Morrow, N. R., and Zhang, X., Generalized Scaling of Spontaneous Imbibition Data for Strongly Water-wet Systems, *Journal of Petroleum Science and Engineering*, Vol. 18, No. 3-4, p. 165-178, 1997.
- MATLAB OptimizationToolbox, Release 2013a, The MathWorks, Inc., Natick, Massachusetts, United States, 2013.
- Mattax, C. C. and KYTE, J. R., Imbibition Oil Recovery from Fractured, Water-drive Reservoir, *SPE Journal*, Vol. 2, No. 2, p. 177-184, 1962.
- Mirzaei-Paiaman, A. and Masihi, M., Scaling Equations for Oil/Gas Recovery from Fractured Porous Media by Counter-Current Spontaneous Imbibition: From Development to Application, *Energy Fuels*, Vol. 27, No. 8, p. 4662-4676, 2013.
- Pirker, B., Mittermeir, G., and Heinemann, Z., Numerically Derived Type Curves for Assessing Matrix Recovery Factors, In Proceedings of EUROPEC/EAGE Conference and Exhibition. Society of Petroleum Engineers, 2007.
- Pooladi-Darvish, M. and Firoozabadi, A., Cocurrent and Countercurrent Imbibition in a Water-wet Matrix Block, *SPE Journal*, Vol. 5, No. 1, p. 3-11, 2000.
- Pordel Shahri, M., Jamialahmadi, M., and Shadizadeh, S. R., New Normalization Index for Spontaneous Imbibition, *Journal of Petroleum Science and Engineering*, Vol. 82, p. 130-139, 2012.
- Putra, E., Fidra, Y., New, I., and Schechter, D. Study of Waterflooding Process in Naturally Fractured Reservoirs from Static and Dynamic Imbibition Experiments, In International Symposium of the Society of Core Analysts. Colorado, 1999.
- Sambridge, M., Geophysical Inversion with a Neighbourhood Algorithm-II. Appraising the Ensemble, *Geophysical Journal International*, Vol. 138, No. 3, p. 727-746, 1999.
- Schembre, J. M. and Kovscek, A. R., Estimation of Dynamic Relative Permeability and Capillary Pressure from Countercurrent Imbibition Experiments, *Transport in Porous Media*, Vol. 65, No. 1, p. 31-51, 2006.

- Schmid, K. S. and Geiger, S., Universal Scaling of Spontaneous Imbibition for Arbitrary Petrophysical Properties: Water-wet and Mixed-wet States and Handy's Conjecture, *Journal of Petroleum Science and Engineering*, Vol. 101, p. 44-61, 2013.
- Skjaeveland, S., Siqveland, L., Kjosavik, A., Thomas, W., and Virnovsky, G., Capillary Pressure Correlation for Mixed-wet Reservoirs, *SPE Reservoir Evaluation, Engineering*, Vol. 3, No. 1, p. 60-67, 2000.
- Zhang, X., Morrow, N., and Ma, S., Experimental Verification of a Modified Scaling Group for Spontaneous Imbibition, *SPE Reservoir Engineering*, Vol. 11, No., 4, p. 280-285, 1996.